Divisome-dependent subcellular localization of cell-cell joining protein SepJ in the filamentous cyanobacterium *Anabaena*

Félix Ramos-León, Vicente Mariscal, José E. Frías, Enrique Flores* and Antonia Herrero

Instituto de Bioquímica Vegetal y Fotosíntesis, CSIC and Universidad de Sevilla, Américo Vespucio 49, E-41092 Seville, Spain

*For correspondence. Tel.: +34954489523; E-mail: eflores@ibvf.csic.es

Running title: Divisome-dependent SepJ localization

This article has been accepted for publication and undergone full peer review but has not been through the copyediting, typesetting, pagination and proofreading process, which may lead to differences between this version and the Version of Record. Please cite this article as doi: 10.1111/mmi.12956

Summary

Heterocyst-forming cyanobacteria are multicellular organisms that grow as filaments that can be hundreds of cells long. Septal junction complexes, of which SepJ is a possible component, appear to join the cells in the filament. SepJ is a cytoplasmic membrane protein that contains a long predicted periplasmic section and localizes to the cell poles in the intercellular septa, but also to a position similar to a Z ring when cell division starts suggesting a relation with the divisome. Here we created a mutant of *Anabaena* sp. strain PCC 7120 in which the essential divisome gene *ftsZ* is expressed from a synthetic NtcA-dependent promoter, whose activity depends on the nitrogen source. In the presence of ammonium, low levels of FtsZ were produced and the subcellular localization of SepJ, which was investigated by immunofluorescence, was impaired. Possible interactions of SepJ with itself and with divisome proteins FtsZ, FtsQ and FtsW were investigated using the bacterial two-hybrid system. We found SepJ self-interaction and a specific interaction with FtsQ, confirmed by co-purification and involving parts of the SepJ and FtsQ periplasmic sections. Therefore, SepJ can form multimers and, in *Anabaena*, the divisome has a role beyond cell division, localizing a septal protein essential for multicellularity.

Introduction

Although bacteria are widely considered as unicellular organisms, there are some cases of true multicellularity. Multicellular bacteria have mechanisms to keep cells together and distinctively exhibit the formation of cells specialized in different functions (Claessen *et al.*, 2014). The heterocyst-forming cyanobacteria are true multicellular

bacteria, and *Anabaena* sp. strain PCC 7120 (hereafter *Anabaena*) is becoming a model to study multicellularity (Flores and Herrero, 2010). *Anabaena* grows as chains of cells (known as filaments or trichomes) that can be hundreds of cells long (Rippka *et al.*, 1979). When *Anabaena* is grown in the absence of combined nitrogen, some photosynthetic vegetative cells in the filament differentiate into N_2-fixing heterocysts (Kumar *et al.*, 2010). In the developed diazotrophic filament vegetative cells and heterocysts exchange nutrients including sugars and amino acids (Wolk *et al.*, 1994; Haselkorn, 2007; Burnat *et al.*, 2014). Heterocyst differentiation requires the global N-control transcription factor NtcA that, under nitrogen deprivation, activates transcription of many genes and represses some others (Herrero *et al.*, 2013). NtcA binds to DNA at sites with consensus sequence $GTAN_8TAC$, which are found in different contexts in regulated promoters. In Class II NtcA-activated promoters, an NtcA-binding site is located about 22 nucleotides upstream from a -10 promoter box in the form TAN_3T (Herrero *et al.*, 2001; Picossi *et al.*, 2014). In *Anabaena*, *ntcA* expression is low when ammonium is present in the growth medium, increases when nitrate is the nitrogen source, and is highest in the absence of combined nitrogen (Muro-Pastor *et al.*, 2002).

The cyanobacteria are diderm bacteria bearing an outer membrane outside of the cytoplasmic membrane and peptidoglycan layers, and in heterocyst-forming cyanobacteria the outer membrane is continuous along the filament, not entering the septa between adjacent cells (Wolk, 1996; Flores *et al.*, 2006; Wilk *et al.*, 2011). Hence, all cells in the filament share a common periplasm (Mariscal *et al.*, 2007). Cell-cell joining structures termed septal junctions (previously known as microplasmodesmata or septosomes) can be observed by transmission electron microscopy and by electron tomography in the intercellular septa (Lang and Fay, 1971; Giddings and Staehelin, 1978; Wilk *et al.*, 2011). These structures appear to be proteinaceous in nature (Wilk *et*

al., 2011). Some genes whose mutation results in filament fragmentation have been identified in *Anabaena*, including the genes in the *fraCDE* operon and *sepJ*, which encode integral membrane proteins that are important for filament integrity mainly under nitrogen deprivation (Bauer *et al.*, 1995; Nayar *et al.*, 2007; Flores *et al.*, 2007; Merino-Puerto *et al.*, 2010). GFP fusions have shown that FraC, FraD and SepJ are located at the intercellular septa, with SepJ being particularly focused in the center of the septum, and that both FraC and FraD are needed for a correct localization of SepJ (Flores *et al.*, 2007; Merino-Puerto *et al.*, 2010). As evidenced by experiments performed with fluorescent tracers, all these proteins influence intercellular molecular exchange in the cyanobacterial filament (Mullineaux *et al.*, 2008; Merino-Puerto *et al.*, 2011).

SepJ, encoded by ORF *alr2338* of the *Anabaena* genome (Kaneko *et al.*, 2001), consists of 751 amino-acid residues and has three well differentiated domains: (i) an N-terminal coiled-coil domain (amino acid residues 28 to 207), which could be involved in protein-protein interactions and is required for proper localization of SepJ at the intercellular septa, filament integrity and diazotrophic growth; (ii) a linker domain rich in Pro and Ser residues (amino acid residues 208 to 410) whose deletion hardly affects SepJ subcellular localization but impairs intercellular transfer of the fluorescent tracer calcein; and (iii) a C-terminal permease (amino acid residues 411 to 751) similar to proteins of the Drug/Metabolite Transporter (DMT) superfamily (Transporter classification database number 2.A.7; http://www.tcdb.org) that appears to be necessary for physiological intercellular molecular exchange (Flores *et al.*, 2007; Mariscal *et al.*, 2011). The coiled-coil and linker domains of SepJ have been predicted to be periplasmic (Flores *et al.*, 2007). In addition to being detected at the cell poles in the intercellular septa as mentioned above, SepJ-GFP is localized to a position similar to

that of a Z ring when cell division starts (Flores *et al.*, 2007; Mariscal and Flores, 2010). The so-called Z ring is made up of the essential tubulin homolog FtsZ at the future site of division in bacteria (Huang *et al.*, 2013).

The divisome is the multiprotein complex responsible for cell division in bacteria (Lutkenhaus *et al.*, 2012; Egan and Vollmer, 2013; Natale *et al.*, 2013). Cyanobacterial cell division genes have been studied by comparative and mutational analyses, which have shown that these organisms contain some cell division genes previously identified in Gram-negative bacteria, some in Gram-positive bacteria, and still some others that are more specific to cyanobacteria (Miyagishima *et al.*, 2005; reviewed in Cassier-Chauvat and Chauvat, 2014). In *Anabaena*, putative divisome genes include *ftsZ* encoding the key Z ring protein (Doherty and Adams, 1995; Zhang *et al.*, 1995), *zipN* (*ftn2*) encoding a possible tether of FtsZ to the cytoplasmic membrane (Koksharova and Wolk, 2002; Marbouty *et al.*, 2009a, 2009b), and *ftsQ* and *ftsW* encoding downstream cytokinetic factors (Vicente *et al.*, 2006). Localization of *Anabaena* FtsZ has been studied using GFP fusions and immunogold labeling, which showed that this protein can form a ring in the middle of dividing cells (Sakr *et al.*, 2006; Klint *et al.*, 2007). FtsZ appears to be at low levels or absent from heterocysts (Kuhn *et al.*, 2000; Klint *et al.*, 2007), but further details on its regulation are unknown.

Similarity between SepJ and FtsZ localization in dividing cells, together with the final localization of SepJ at the cell poles, suggests that SepJ might be recruited to the division ring and interact with proteins of the divisome. In this work, we addressed the localization of SepJ in a conditional *ftsZ* mutant of *Anabaena*, which expresses different levels of FtsZ depending on the nitrogen source. We found that SepJ localization is impaired when *ftsZ* expression is down regulated resulting in low cellular levels of the FtsZ protein. Moreover, using the bacterial two-hybrid system, we found evidence for

SepJ self-interactions and an interaction between SepJ and *Anabaena* FtsQ, a protein that is known to recruit several downstream divisome elements. This interaction could be confirmed by co-purification of both proteins expressed in *Escherichia coli*. Our data suggest the formation of SepJ multimers and identify a role of the divisome beyond cell division, contributing to the assembly of the supracellular structure of a bacterial pluricellular filament.

Results

Construction of a strain with NtcA-dependent expression of ftsZ

The *ftsZ* gene is located 1,191 bp downstream of *ftsQ* in the *Anabaena* chromosome (Kaneko *et al.*, 2001). There is no evidence for co-transcription of the two genes, and *ftsZ* is expressed at higher levels than *ftsQ* (Flaherty *et al.*, 2011). To create a conditional mutant of the essential *ftsZ* gene in *Anabaena*, we designed a construct in which *ftsZ* was expressed from a synthetic NtcA-dependent promoter, which we will denote P_{ND}. This promoter was designed based on known features of Class II NtcA-activated promoters (Herrero *et al.*, 2001) and contains a consensus NtcA-binding site located 23 bp upstream from a -10 promoter box (Fig. 1A). The P_{ND} promoter, together with the C.S3 gene cassette, was inserted in the *Anabaena* chromosome 5' of nucleotide 52 upstream of the *ftsZ* start codon (see Fig. 1A and Experimental procedures for details). An *Anabaena* clone containing only chromosomes bearing the C.S3-P_{ND} construct was named strain CSFR18 (Fig. S1).

Because NtcA-dependent promoters are most active when the cells are incubated in the absence of a source of combined nitrogen and least active in the presence of ammonium, strain CSFR18 was expected to grow well diazotrophically and, as a consequence of insufficient *ftsZ* expression, poorly in the presence of ammonium. Tests

of growth on solid medium showed poorer growth in the presence of ammonium than fixing N_2 or in the presence of nitrate (Fig. 1B). Strain CSFR18 was therefore routinely maintained on solid BG11 (nitrate-containing) medium. When CSFR18 cells grown on BG11 medium were inoculated in liquid medium, growth was observed for about 5 days independently of the nitrogen source. Although the growth rates were somewhat slower than those of the wild type, exponential growth was not much affected (Fig. S2). Microscopic inspection of the cultures showed, however, an altered morphology, mainly in ammonium-containing media, in which the mutant cells were significantly larger than the wild-type cells (Fig. 1C). In contrast to many bacteria in which lack of FtsZ results in cell elongation (Margolin, 2009), the cylindrical *Anabaena* cells got enlarged, being longer and wider than the control cells, in response to decreased expression of *ftsZ*. In the presence of nitrate the cells of the mutant were also larger than the wild-type cells, but in the diazotrophic cultures mutant and wild-type cells were similar in size (cellular areas are summarized in the legend to Fig. 1). The final appearance of the cultures was very different as observed after 7 days of incubation under the different nitrogen regimes (Fig. 1D). The culture of the mutant containing nitrate as the nitrogen source was yellowish, which is indicative of an altered physiology, the culture with ammonium was largely lysed (hence the lack of turbidity and the blue color reflecting the release of phycobiliproteins from the cells), and only the diazotrophic culture was similar to the corresponding wild-type culture.

The observations described above are consistent with NtcA-dependent expression of *ftsZ* in strain CSFR18, with a limited expression mainly in ammonium-containing cultures. Transcript levels of *ftsZ* were determined after two days of incubation in liquid medium with the different nitrogen sources. Levels of *ftsZ* transcript were about 23%, 60% and 89% in the mutant as compared to the wild type in

media containing ammonium, nitrate or no combined nitrogen, respectively (Fig. 2A). The low level of *ftsZ* expression in cells of CSFR18 incubated in the presence of ammonium corroborates that the P_{ND} promoter substitutes for the natural *ftsZ* promoter in this strain. Our results also show that in the wild type, *ftsZ* expression is about 2-fold higher in the diazotrophic cultures than in cultures containing combined nitrogen. Western blot analysis performed with an antibody raised against the FtsZ protein of *Anabaena* expressed in *E. coli* confirmed that the FtsZ levels in strain CSFR18 were higher in diazotrophic than in nitrate-containing cultures, and lowest in ammonium-containing cultures, with the levels in the absence of combined nitrogen being similar in the mutant and the wild type (Fig. 2B).

Subcellular localization of FtsZ in the wild type and strain CSFR18 was addressed by immunofluorescence with the *Anabaena* FtsZ antibodies. In the wild type, localization of FtsZ in a ring at the middle of the cells could be readily observed in vegetative cells, but not in heterocysts (Fig. 3). (We repeatedly found poor labeling in ammonium-grown wild-type cells, but the reason for this is unknown.) In strain CSFR18, FtsZ ring labeling was readily observed in diazotrophic filaments, in which a number of vegetative cells, but not heterocysts, were labeled (Fig. 3). In this strain, an FtsZ ring was observed with difficulty in some cells of the filaments incubated with nitrate, but it was not observed in the big cells produced after incubation in the presence of ammonium. These results are consistent with the different levels of FtsZ observed by western blot analysis in the cells of CSFR18 incubated with different nitrogen sources.

SepJ localization in strain CSFR18

Once a strain with regulated expression of *ftsZ* was available and conditions leading to production of low FtsZ cellular levels were established, we addressed the localization of

SepJ under those conditions. Localization of SepJ has previously been investigated using a SepJ-GFP fusion (Flores *et al.*, 2007; Mariscal *et al.*, 2011). For this work, however, we set up a protocol to study the subcellular localization of the native SepJ protein by immunofluorescence, using antibodies raised against the coiled-coil domain of SepJ (anti SepJ-CC antibodies; Mariscal *et al.*, 2011). These antibodies localized SepJ at the cell poles in filaments grown with nitrate as the nitrogen source (Fig. 4). Additionally, SepJ was observed, less focused, in the middle of enlarged cells that were apparently dividing (see N_2-grown cells in Fig. 4).

In strain CSFR18, specific localization of SepJ at the cell poles was only observed in filaments that had been incubated without combined nitrogen (Fig. 4). In filaments incubated for 2 days in ammonium-containing medium, the SepJ signal, seen as spots, was delocalized. In filaments incubated with nitrate, SepJ could be observed localized in the cell poles, but also some SepJ signal was observed disperse (Fig. 4 and not shown). Because of the low levels of FtsZ protein present in the cells incubated with ammonium, these observations suggest that the correct localization of SepJ at the cell poles needs the presence of FtsZ in the cells at normal, or close to normal, levels.

Treatment with berberine

Berberine is a plant alkaloid that has been shown to interfere with the assembly of the FtsZ ring (Domadia *et al.*, 2008; Boberek *et al.*, 2010). To assess in a different way the possible role of FtsZ in the localization of SepJ, we treated *Anabaena* cells with berberine and performed immunofluorescence tests with the anti FtsZ and anti SepJ-CC antibodies. Incubation of cells grown using nitrate as the nitrogen source with 0.1 mM berberine for 24 h hampered the formation of the FtsZ ring (Fig. 5). Longer incubations ($\geq$ 48 h) or incubation with higher berberine concentrations ($\geq$ 0.2 mM) resulted in cell

lysis. The filaments with cells lacking an FtsZ ring showed SepJ labeling more spaced than the non-treated filaments (Fig. 5). Mean distance between SepJ spots was 3.0 ± 0.7 μm (number of intervals counted, n = 76) in untreated filaments and 5.1 ± 2.5 μm (n = 74) in berberine-treated filaments (the significance of the difference between untreated and treated filaments was assessed by the Student's *t* test; $P < 10^{-10}$). Whereas spots observed with the anti SepJ-CC antibodies may correspond to SepJ proteins placed at the intercellular septa before the treatment with berberine, implying a remarkable stability of SepJ, elongated cells in which no SepJ signal is evident may result from lack of SepJ localization related to lack of FtsZ assembly. Although indirect effects of berberine cannot be ruled out, these results are consistent with a dependence of SepJ localization on the FtsZ ring as deduced above with the CSFR18 mutant.

Protein-protein interactions tested with the bacterial two-hybrid system

The dependence of SepJ subcellular localization on FtsZ could result from a direct interaction between these two proteins or from an interaction of SepJ with other protein(s) of the divisome that require FtsZ for proper localization. To identify possible direct interactions of SepJ with FtsZ or some other divisome proteins, we used the bacterial two-hybrid system (BACTH), which permits a visual screening for interactions on X-gal-containing plates and an estimation of the strength of those interactions by quantitative determination of β-galactosidase activity (Karimova *et al.*, 1998). Fusions of SepJ and divisome proteins FtsZ, FtsQ and FtsW, all of them from *Anabaena*, to the two complementary fragments (T18 and T25) of the catalytic domain of adenylate cyclase were prepared and cloned together in different combinations. The predicted topology of the protein fusions used is schematized in Fig. 6, and β-galactosidase activities are presented in Table 1.

We first checked whether SepJ interacts with itself by cloning SepJ fused to the N-termini of T25 (SepJ-T25) and T18 (SepJ-T18). Whereas appropriate control combinations with empty T18 or T25 plasmids were negative, a strong interaction was detected for the SepJ-T25/SepJ-T18 pair (Table 1). This result shows that SepJ can be involved in protein-protein interactions when fused to either T18 or T25. As described in the Introduction, *Anabaena* SepJ bears three well-defined domains: a coiled-coil domain and a linker domain that likely reside in the periplasm and an integral membrane (permease) domain (schematically depicted in Fig. 6). To test a possible role of specific protein domains in the interaction, we prepared truncated versions of SepJ lacking (i) a substantial part (amino acid residues 463 to 748, leaving only one putative transmembrane segment) of the permease domain, denoted SepJ(ΔTM), (ii) most of the predicted periplasmic section, including both the coiled-coil and linker domains (amino acid residues 40 to 410), denoted SepJ(Δpp), (iii) the linker domain (amino acid residues 223 to 410), denoted SepJ(Δlinker), and (iv) most of the coiled-coil domain (amino acid residues 40 to 201), denoted SepJ(ΔCC). These proteins were fused to the N-termini of T25 and T18, and appropriate controls of interaction with empty T18 and T25, respectively, were negative (Table 1). SepJ(ΔTM) did not show self-interaction or interaction with the whole SepJ, and SepJ(Δpp) showed a very low self-interaction and no interaction with the whole SepJ (Table 1). In contrast, SepJ(Δlinker) and SepJ(ΔCC) showed weak and strong self-interactions, respectively, and appreciable interactions with the whole SepJ in both cases. Because SepJ is a cytoplasmic membrane protein, it is possible that the truncated SepJ(ΔTM) protein is not properly incorporated into the membrane making any interaction not possible. In contrast, interactions observed with SepJ(Δlinker) and SepJ(ΔCC) indicate that these proteins were properly produced to

work appreciably. These results show an important role of the linker domain in SepJ self-interactions.

The SepJ-T18 plasmid (or the T18 plasmid as a control) was then tested with FtsZ-T25 (FtsZ fused to the N-terminus of T25), T25-FtsW (FtsW fused to the C-terminus of T25), and T25-FtsQ (FtsQ fused to the C-terminus of T25) (see schemes in Fig. 6). Whereas all controls with empty T18 were negative, in the SepJ-divisome protein pairs tested no interaction was detected with FtsZ, a weak interaction of uncertain statistical significance was detected with FtsW, and a strong interaction was detected with FtsQ (Table 1). Whereas the negative result with FtsZ does not provide evidence for interaction and the result with FtsW leaves the possibility of an interaction open, the positive result with FtsQ suggests interaction of this protein with SepJ.

FtsQ from *E. coli* has one transmembrane segment and a periplasmic section consisting of two domains, α and β, that mediate interactions with other proteins (Chen *et al.*, 1999; van den Ent *et al.*, 2008; Villanelo *et al.*, 2011), and *Anabaena* FtsQ is predicted to have similar domains (Fig. S3). To investigate possible domain-specific interactions of SepJ with FtsQ, the SepJ truncated proteins were tested. Whereas SepJ(ΔTM) and SepJ(Δlinker) did not interact, and SepJ(Δpp) showed a very weak interaction with FtsQ, SepJ(ΔCC) showed a strong interaction (Table 1). Whereas, as noted above, lack of proper integration of SepJ(ΔTM) into the cytoplasmic membrane cannot be ruled out, these results suggest a role of the SepJ linker domain in interaction with FtsQ.

To test whether one or the two of the FtsQ periplasmic domains have a role in interaction with SepJ, we prepared truncated versions of FtsQ, FtsQ(Δα) and FtsQ(Δβ) (Fig. S3), fused to the C-terminus of T25. Whereas control tests with T18 were negative, tests with SepJ-T18 showed a very weak interaction with FtsQ(Δα) and a very

strong interaction with FtsQ(Δβ), suggesting that the α domain, but not the β domain is needed for the FtsQ-SepJ interaction.

Co-purification of SepJ and FtsQ

To corroborate the interaction of SepJ and FtsQ, an *E. coli* strain carrying compatible plasmids expressing SepJ-GFP and His_6-FtsQ, respectively, was prepared. Because a part of the predicted periplasmic section of SepJ appears necessary for the interaction, a plasmid expressing a SepJ-GFP fusion protein without most of this section (Δpp-SepJ-GFP) was also used. As controls, *E. coli* strains with a plasmid expressing one of the proteins (SepJ-GFP, Δpp-SepJ-GFP or His_6-FtsQ) and the second plasmid without an insert were constructed. Cell-free extracts were prepared by breaking down the cells in a French pressure cell (see Experimental procedures), incubated with anti GFP antibodies (anti-GFP MicroBeads) and passed through a magnetic-activated cell sorting (MACS) column, and the material retained was eluted and subjected to SDS-PAGE. It should be noted that the material retained in the column should consist of inside-out membrane micro-vesicles (normally produced by French pressure cell breakage; see e.g., Altendorf and Staehelin, 1974), in which the cytoplasmic-exposed GFP is available for interaction with the antibodies. As shown in Fig. 7A, His_6-FtsQ, detected with anti His-tag antibodies, was retained in the case of extracts containing also SepJ-GFP, but much less in those containing Δpp-SepJ-GFP or not in the case of control extracts lacking SepJ. The presence of SepJ-GFP or Δpp-SepJ-GFP in the corresponding preparations was corroborated with anti-GFP antibodies (Fig. 7B). These results indicate that FtsQ was recovered at substantial levels only in micro-vesicles containing the whole SepJ protein, thus corroborating an interaction of SepJ with FtsQ that requires the predicted periplasmic section of SepJ to take place.

Discussion

SepJ is a key protein in *Anabaena* multicellularity, since mutants lacking SepJ show a strong filament fragmentation phenotype (Nayar *et al.*, 2007; Flores *et al.*, 2007) and are impaired in the intercellular transfer of a fluorescent tracer (Mullineaux *et al.*, 2008; Mariscal *et al.*, 2011). SepJ-GFP fusions have been shown to localize to the cell poles at the intercellular septa in the filaments of *Anabaena* (Flores *et al.*, 2007; Mariscal *et al.*, 2011), and immunofluorescence analysis performed in this work with an antibody raised against the coiled-coil domain of *Anabaena* SepJ has confirmed the same localization for native SepJ (Fig. 4). This same approach has recently permitted the localization of SepJ in the complex intercellular septa of the true-branching, heterocyst-forming filamentous cyanobacterium *Mastigocladus laminosus* (Nürenberg *et al.*, 2014), indicating that localization of SepJ at the intercellular septa may be a universal feature in heterocyst-forming cyanobacteria.

In contrast to SepJ-GFP, which is observed as a single fluorescence spot in the septa between adjacent vegetative cells (Flores *et al*., 2007), two spots, one in each of the adjacent cells, are frequently observed in the immunofluorescence analysis (Fig. 4) indicating that SepJ localizes to both poles in each cell. Two spots have also been observed in immunofluorescence analysis with anti-GFP antibodies in a strain producing SepJ-GFP (Mariscal and Flores, 2010). (The two foci at the intercellular septa likely result from shrinking of the cells during preparation for immunofluorescence that involves a dehydration step.) Therefore, to produce a single fluorescence spot from the SepJ-GFP fusion, in which the GFP is predicted to reside next to the cytoplasmic face of the cytoplasmic membrane (Flores *et al.*, 2007), SepJ from adjacent cells must be very close to each other. On the other hand, our BACTH

analysis has unraveled a strong self-interaction of SepJ, for which the linker domain appears to be very important, indicating that SepJ can form multimers in the cells producing it. All these observations are consistent with the idea that SepJ is part of a septal junction complex in which SepJ multimers from adjacent cells interact, presumably through the SepJ coiled-coil domains that, as described previously (Mariscal *et al.*, 2011), are required to keep SepJ at the cell poles.

SepJ-GFP is also seen to localize in a ring, similar to a Z ring, when cell division starts (Flores *et al.*, 2007; Mariscal and Flores, 2010), and a related location has also been confirmed here for native SepJ by immunofluorescence (Fig. 4). Localization in a Z ring and progressive focusing to the new cell poles as the septum is synthesized during cell division suggested a relation with the divisome. Because *ftsZ* is an essential gene in most bacteria including *Anabaena* (Zhang *et al.*, 1995), we constructed strain CSFR18 in which, based on expression from a synthetic NtcA-dependent promoter, the FtsZ levels depend on the provided nitrogen source. This strain produces very low levels of FtsZ after incubation for a few days in the presence of ammonium, resulting in malformed cells that eventually lyse. However CSFR18 can be maintained in the presence of nitrate, although the highest levels of FtsZ, similar to the wild-type levels and readily seen to form a Z ring, are observed in the vegetative cells of diazotrophic filaments. Thus, we could study the localization of SepJ, tested by immunofluorescence, as a function of FtsZ abundance in filaments of strain CSFR18 grown with nitrate and incubated for a few days in medium with nitrate, ammonium or lacking a source of combined nitrogen. Our results show that the correct localization of SepJ requires the presence of close to normal FtsZ levels, which are best attained in the diazotrophic filaments of strain CSFR18 (Fig. 4). In a complementary approach, we observed that treatment of *Anabaena* cells with berberine impedes FtsZ ring formation, as previously

shown for *E. coli* (Domadia *et al.*, 2008; Boberek *et al.*, 2010), and affects the correct localization of SepJ. All these results together suggest that FtsZ has a role in the subcellular localization of SepJ.

Dependence of SepJ localization on FtsZ can be indirect, since FtsZ has a scaffolding role for the divisome. We therefore addressed, using BACTH, the possible direct interaction of SepJ with FtsZ and two downstream divisome proteins, FtsQ and FtsW, all of them from *Anabaena*. A strong interaction was observed only between SepJ and FtsQ, consistent with FtsQ recruiting SepJ to the divisome, which is reminiscent of the FtsQ role in *E. coli* at recruitment of downstream cell division proteins (Chen *et al.*, 2002). The interaction between SepJ and FtsQ could be confirmed by co-purification of the two proteins expressed in *E. coli* (Fig. 7), which also showed a role of the predicted periplasmic section of SepJ in this interaction. This is consistent with the results of BACTH analysis, which suggest a role of the linker domain of SepJ in a specific interaction with the periplasmic α domain of FtsQ. This domain exhibits high similarity to polypeptide transport-associated (POTRA) domains (van den Ent *et al.*, 2008). Although we cannot rule out that interactions between the transmembrane segments of these proteins occur, our results support a specific interaction between parts of the long extra-membrane section of SepJ and the periplasmic section of FtsQ. A corollary of this observation is that the section of SepJ containing the coiled-coil and linker domains is periplasmic, as predicted previously (Flores *et al.*, 2007). We therefore suggest that SepJ localization at the cell poles in the intercellular septa depends on the divisome, involving an interaction with FtsQ. Nonetheless, interactions of SepJ with other divisome proteins may also take place, some of which may be functionally redundant as is not uncommon in interactions between divisome proteins (Lutkenhaus *et al.*, 2012). A more ample analysis of interactions between SepJ and

390 divisome proteins will need however an increased knowledge of the *Anabaena*
391 divisome. Localization of SepJ at the cell poles may additionally be stabilized by the
392 above-discussed interactions between the coiled-coil domains of SepJ proteins from
393 adjacent cells.

394 In filamentous cyanobacteria, when cell division is completed, the peptidoglycan
395 layers of the two adjacent cells remain fused in a substantial number of the filament's
396 septa allowing the isolation of murein sacculi corresponding to several cell units
397 (Lehner *et al.*, 2011), and the outer membrane does not enter into the septum between
398 adjacent cells (Wolk, 1996; Flores *et al.*, 2006; Wilk *et al.*, 2011). Thus, the divisome of
399 this type of cyanobacteria must differ in composition and/or regulation of its activity
400 from the divisome of unicellular bacteria, including unicellular cyanobacteria, which
401 performs splitting of septal peptidoglycan and invagination of the outer membrane to
402 complete cell division. Because SepJ or a SepJ-like protein is found in most filamentous
403 cyanobacteria (Mariscal *et al.*, 2011; Nürenberg *et al.*, 2014), an interaction of SepJ
404 with the divisome might contribute to the characteristic cell division of these organisms.
405 Besides SepJ, the *fraCDE* operon is often conserved in filamentous cyanobacteria
406 (Merino-Puerto *et al.*, 2013), and products of this operon have also been observed in the
407 place of the Z ring (FraC, observed with a FraC-GFP fusion; Merino-Puerto *et al.*,
408 2010) or in the growing intercellular septa (FraD, observed by means of immunogold
409 labeling; Merino-Puerto *et al.*, 2011), making it possible that these proteins interact with
410 the divisome as well. Specific late events during cell division may be at the basis of the
411 multicellular character of these bacteria, in which the divisome appears to have a role
412 localizing proteins essential for multicellularity.
413
414

Experimental procedures

Strains and growth conditions

Anabaena sp. strain PCC 7120 (also known as *Nostoc* sp. strain PCC 7120) and strain CSFR18 were grown in BG11 (containing $NaNO_3$), $BG11_0$ (free of combined nitrogen) or $BG11_0$ + ammonium ($BG11_0$ containing 4 mM NH_4Cl and 8 mM TES-NaOH buffer, pH 7.5) media at 30ºC in the light (25 μE m^{-2} s^{-1} from fluorescent lamps), in shaken (80-90 rpm) liquid cultures or in medium solidified with 1% Difco agar. The BG11-based medium contained ferric citrate instead of the ferric ammonium citrate used in the original recipe (Rippka *et al.*, 1979). Media for strain CSFR18 was supplemented with 5 μg ml^{-1} streptomycin sulfate (Sm) and 5 μg ml^{-1} spectinomycin dihydrochloride pentahydrate (Sp).

Escherichia coli DH5α and XL1-Blue (Stratagene) were used for plasmid constructions. Strains HB101 and ED8654 were used for conjugation with *Anabaena*. Strain BTH101 (*cya*-99) was used for BACTH analysis. Strain BL21-lacIq was used for production of *Anabaena* FtsZ and co-purification assays. All *E. coli* strains were grown in LB medium, supplemented when appropriate with antibiotics at standard concentrations (Ausubel *et al.*, 2014; Karimova *et al.*, 2005).

Plasmid construction and genetic procedures

DNA was isolated from *Anabaena* sp. by the method of Cai and Wolk (1990). Plasmid pCSFR15, carrying *ftsZ* (ORF *alr3858*) under the control of the synthetic NtcA-regulatable promoter, P_{ND}, was prepared by PCR and standard cloning procedures. pCSFR15 is a pMBL-based plasmid that contains a fragment upstream of *alr3858* (*Anabaena* chromosome coordinates 4,655,349 to 4,655,844), amplified by PCR using primers alr3858-3 and alr3858-4 (all oligodeoxynucleotide primers are described in

441 Table S1) and cloned between ApaI and SalI sites; the C.S3 cassette (Elhai and Wolk,
442 1988; C.S3 is derived from the Ω cassette described by Prentki and Krisch, 1984)
443 cloned into BamHI; a synthetic NtcA-regulated promoter generated by PCR using Pro-
444 sNtcA-1 and Pro-sNtcA-2 overlapping primers and cloned into SpeI and EcoRV sites;
445 and the 5' region of *alr3858* (coordinates 4,655,850 to 4,656,703), amplified by PCR
446 using primers alr3858-1 and alr3858-2 and cloned between SacI and XhoI sites. The
447 insert of pCSFR15 was corroborated by sequencing and digested with PvuII, and the
448 fragment containing the C.S3-P_{ND} construct was transferred to pRL278 previously
449 digested with XhoI and treated with the Klenow fragment producing pCSFR18. This
450 plasmid was transferred by conjugation, performed as described (Elhai *et al.*, 1997), to
451 *Anabaena* sp. strain PCC 7120 with selection for resistance to Sm and Sp. Cultures of
452 exconjugants obtained were used to select for clones resistant to 5% sucrose (Cai and
453 Wolk, 1990), and individual Suc^R colonies were checked by PCR. Clones in which the
454 C.S3-P_{ND} construct was inserted into *ftsZ* upstream region were isolated, and a clone
455 homozygous for the chromosomes bearing this construct was selected for further
456 analysis and named strain CSFR18.
457 For bacterial two-hybrid (BACTH) analysis, all genes were amplified using
458 *Anabaena* DNA as template. The following primers were used: all0154-9 and all0154-
459 10 to amplify *ftsW* (ORF *all0154*); alr3857-7 and alr3857-8 to amplify *ftsQ* (ORF
460 *alr3857*); and alr3858-13 and alr3858-14 to amplify *ftsZ*. The PCR products
461 corresponding to *alr0154* and *alr3857* were cloned in pKT25 using PstI and BamHI,
462 and that corresponding to *alr3858* was cloned in pKNT25 using the same enzymes. For
463 the *sepJ* gene (ORF *alr2338*), a PCR product amplified using alr2338-13 and alr2338-
464 35 primers was cloned in pCSVM97 (bearing the complete *sepJ* gene with the stop
465 codon substituted by a XhoI restriction site; unpublished) using PstI and XbaI,

generating plasmid pCSE216. The pCSE216 insert was then transferred to pUT18 and pKNT25 using PstI and SmaI. In addition, primers alr2338-35 and alr2338-36 were used to amplify *sepJ*-truncated versions using genomic DNA from *Anabaena* strains CSVM25, CSVM26, CSVM85 (Mariscal *et al.*, 2011) and CSVM90 (bearing a *sepJ* gene encoding a SepJ protein lacking amino acid residues 463 to 748; unpublished). The resulting PCR products were cloned in pUT18 and pKNT25 using PstI and SmaI and sequenced. As a result, the following plasmids were generated: pCSFR30 (producing T25-FtsQ), pCSFR31 (producing T25-FtsW), pCSFR32 (producing FtsZ-T25), pCSE221 (producing SepJ-T18), pCSE222 (producing SepJ-T25), pCSE226 (producing SepJ_CSVM25-T18), pCSE227 (producing SepJ_CSVM26-T18), pCSE228 (producing SepJ_CSVM90-T18), pCSE231 (producing SepJ_CSVM25-T25), pCSE236 (producing SepJ_CSVM90-T25), pCSE237 (producing SepJ_CSVM26-T25), pCSE239 (producing SepJ_CSVM85-T18) and pCSE240 (producing SepJ_CSVM85-T25). For simplicity, SepJ_CSVM25 is denoted SepJ(ΔCC), SepJ_CSVM26 is denoted SepJ(Δpp), SepJ_CSVM85 is denoted SepJ(Δlinker), and SepJ_CSVM90 is denoted SepJ(ΔTM).

Also for BACTH analysis, to produce a version of *Anabaena* FtsQ with the α domain deleted, two DNA fragments, one encoding amino acid residues 1 to 59 and the other one residues 128 to 281, were amplified by PCR using primer pairs alr3857-7/alr3857-10 and alr3857-11/alr3857-8 respectively. Both DNA fragments were used as template in an overlapping PCR using primers alr3857-7 and alr3857-8. The fragment obtained was digested with PstI and BamHI and inserted into pKT25 with the same enzymes producing pCSFR45, which encodes FtsQ(Δα) fused to the C terminus of the T25 subunit. To produce a version of *Anabaena* FtsQ lacking the β domain (lacking amino acid residues 128 to 281) and fused to the C-terminus of the T25 subunit, a DNA

491 fragment obtained by PCR using primers alr3857-7 and alr3857-9 (which includes a
492 termination codon) was cloned in pKT25 using PstI and BamHI. This plasmid was
493 called pCSFR46.

494 To produce *Anabaena* FtsZ protein and obtain an antibody against it, the *ftsZ*
495 gene was amplified using *Anabaena* DNA as template and primers alr3858-7 and
496 alr3858-8, and the PCR product was cloned in vector pCOLADuet-1 (Novagen) using
497 BamHI and XhoI, producing plasmid pCSFR22.

498 For co-purification assays, plasmids bearing genes encoding GFP-tagged SepJ
499 (or GFP-tagged SepJ without most of its predicted periplasmic section, denoted Δpp-
500 SepJ-GFP) and His-tagged FtsQ were constructed. The *Anabaena ftsQ* gene was
501 amplified using primers alr3857-13 and alr3857-14, and the PCR product was digested
502 with BamHI and XhoI and cloned in pACYCDuet (Novagen) using the same enzymes,
503 producing plasmid pCSFR50 (six histidine residues added to the N terminus of FtsQ).
504 To produce SepJ-GFP and Δpp-SepJ-GFP a SacI-EcoRI fragment from pCSAL33
505 (bearing the *gfp-mut2* gene; A. López-Lozano and A. Herrero) was cloned in pCSE221
506 or in pCSE227, producing pCSFR51 and pCSFR52 respectively.

507

508 *Expression and purification of* Anabaena *FtsZ*

509 Plasmid pCSFR22, which contains the *Anabaena ftsZ* gene fused to a sequence
510 encoding a His_6 tag under an IPTG-inducible promoter, was transferred to *E. coli* BL21-
511 lacIq. A pre-inoculum of this strain grown overnight in LB medium supplemented with
512 50 μg of kanamycin sulfate (Km) ml^{-1} and 2% glucose was washed with LB medium
513 and used to inoculate 1 L of LB medium + Km. The culture was incubated at 37ºC up to
514 an OD_{600} of 0.6. Protein expression was induced by addition of 1 mM isopropyl-β-D-1-
515 thiogalactopyranoside (IPTG). After 3 h at 37ºC, cells were collected and resuspended

516 in a buffer containing 50 mM Tris-HCl (pH 8.0), 200 mM NaCl and 10% glycerol (5
517 ml/g of cells). DNaseI and protease inhibitor cocktail *complete Mini EDTA-free* (Roche)
518 were added just before breakage of the cells by passage twice through a French pressure
519 cell at 20,000 psi. After centrifugation at 15,000 *g* (10 min, 4ºC), the His_6-FtsZ protein
520 was purified from the supernatant by chromatography through a 5-ml His-Select column
521 from Sigma, using imidazole to elute the retained proteins. Samples obtained after
522 purification were subjected to SDS-PAGE, excised from the gel, electro-eluted and
523 concentrated (Stirred Ultrafiltration Cell, Millipore). An amount of 1.4 mg of purified
524 protein was used in subcutaneous injection of a rabbit to produce antibodies in the
525 'Centro de Producción y Experimientación Animal', Universidad de Sevilla (Seville,
526 Spain). Antiserum was recovered 90 days after the first injection and stored at -80ºC
527 until used.
528
529 *Protein sample preparation and western blots*
530 Samples containing 5 μg of chlorophyll *a* were taken from cultures of *Anabaena* strains
531 incubated in the presence of different nitrogen sources for 48 h. Total proteins were
532 precipitated by incubating samples in 10% trichloroacetic acid at 4ºC for at least 30
533 min, subsequent centrifugation at 13,200 *g* (4ºC, 30 min) and finally washed with cold
534 acetone. The protein pellet was dried for 15 min and then resuspended in a buffer
535 containing 50 mM Tris-HCl (pH 7.5), 50 mM NaCl and 10% glycerol. After that,
536 samples were mixed with 1 volume of 2x sample buffer, incubated at 95ºC for 15 min,
537 run in a 10% Laemmli SDS-PAGE system, and transferred to PVDF membrane filters
538 as previously reported (Mariscal *et al.*, 2011). For detection of *Anabaena* FtsZ, the
539 filters were incubated overnight in blocking buffer containing 10 mM Tris-HCl (pH
540 7.5), 150 mM NaCl, 5% non-fat milk powder and 0.05% Tween-20. Afterwards,

primary anti-FtsZ serum (diluted 1:1000 in blocking buffer) was added, incubated at 30ºC for 1 h and washed three times with TBS. Secondary antibody (anti-rabbit IgG conjugated to peroxidase from Sigma) was then added at a dilution 1:10,000 in blocking buffer, incubated 1 h at 30ºC and washed three times with TBS. Detection was performed with a chemiluminiscence kit (WesternBright™ ECL, Advansta) and exposure to hyperfilm (GE Healthcare).

For co-purification assays, *E. coli* strains expressing *Anabaena* FtsQ fused to a His_6 tag and SepJ or Δpp-SepJ fused to GFP, or control plasmid vectors, were induced with IPTG as described above. After 4 h at 37ºC, cells were collected and resuspended in 5 mL of PBS containing 140 mM NaCl, 1.5 mM KH_2PO_4, 2.7 mM KCl (pH 7.4) and one tablet of protease inhibitor cocktail *complete Mini EDTA-free* (Roche). Cells were disrupted by passage twice through a French pressure cell at 20,000 psi. After centrifugation at 15,000 *g* (10 min, 4ºC), cell extracts were incubated with μMACS Anti-GFP MicroBeads (Miltenyi Biotec) for 1 h. Afterwards, the mixture was loaded into a MACS column (Miltenyi Biotec) and the column was washed with 3 mL of PBS buffer. Elution of the GFP-tagged protein (SepJ or Δpp-SepJ) and its interacting protein(s) was accomplished with buffer containing 50 mM Tris-HCl (pH 6.8), 50 mM DTT, 1% SDS, 1 mM EDTA, 0.005% bromphenol blue and 10% glycerol. The eluate was subjected to electrophoresis in a 10% Laemmli SDS-PAGE system. SepJ-GFP and Δpp-SepJ-GFP were detected by western blot as described above using an anti-GFP antibody (A6455 from Invitrogen) diluted 1:2,000. His_6-tagged FtsQ was detected using anti-His HRP-conjugated antibody (Qiagen) following the instructions from the supplier.

Growth rates

The growth rate, μ, which corresponds to $\ln 2/t_d$, where t_d is the doubling time, was calculated from the increase of protein concentration determined by a modified Lowry procedure (Markwell *et al.,* 1978) in 0.2-ml samples from shaken cultures. The growth rate was followed for a period of 5 days, between cellular densities corresponding to 5 to about 100 μg of protein (0.2-4 μg of chlorophyll *a*) per ml. Chlorophyll *a* content of cultures was determined by the method of Mackinney (1941).

Analysis of ftsZ *expression by RT-qPCR*

RNA was isolated as described previously (Mohamed and Jansson, 1989) from cultures of *Anabaena* strains incubated in the presence of different nitrogen sources. RNA (100 ng) was used for retrotranscription using Quantitect Reverse Transcription Kit (Qiagen). cDNA obtained was used to carry out real time PCR using *iCycler iQ Real Time PCR Detection System* equipped with the *iCycler iQ* v 3.0 software from BioRad. PCR amplification was carried out using SensiFAST™ SYBR & Fluorescein Kit (BioLine) following the instructions from the supplier. The amplification protocol was as follows: 1 cycle at 95ºC for 2 min, 30 cycles of: 95ºC for 15 s, 67ºC for 20 s and 72ºC for 30 s. After this protocol was ended, a melting point calculation protocol was done in order to check that only the correct product was amplified in each tube. The expression of *alr0599* and *all5167* (Flaherty *et al.,* 2011) was used as internal standards to normalize the values obtained for *alr3858* (*ftsZ*). To study expression of these genes, the following primer pairs were used: alr0599-1/alr0599-2, all5167-1/all5167-2, and alr3858-9/alr3858-10, respectively.

The mathematical treatment of data to calculate relative gene expression was performed according to Pfaffl (2001) using the formula: Relative gene expression = $2^{-\Delta\Delta Ct}$. Where ΔΔCt corresponds to the increase in the threshold cycle of the problem

591 gene with respect to the increase in the threshold cycle of the housekeeping genes
592 (*alr0599* and *all5167*). The final quantification value for each condition indicates the
593 relative change of gene expression in strain CSFR18 and the wild type with respect to
594 the wild-type strain grown with nitrate as nitrogen source.
595
596 *Immunolocalization and fluorescence microscopy*
597 For immunolocalization of SepJ or FtsZ, cells from 1.5 ml of liquid cultures were
598 collected by centrifugation, placed atop a poly-L-lysine pre-coated microscope slide and
599 covered with a 45-μm pore-size Millipore filter. Afterwards, the filter was removed and
600 the slide was let to dry at room temperature and, then, immersed in 70% ethanol
601 at -20ºC for 30 min and dried 15 min at room temperature. The cells were washed twice
602 (2 min each time, room temperature) by covering the slide with PBS-T (PBS
603 supplemented with 0.05% Tween-20). Subsequently, the slides were treated with a
604 blocking buffer (5% milk powder in PBS-T) for 15 min. Cells on the slides were then
605 incubated with a primary antibody (anti-SepJ-CC [Mariscal *et al.*, 2011], diluted in
606 blocking buffer 1:250, or anti-FtsZ serum, diluted 1:100) for 90 min, washed three
607 times with PBS-T, incubated 45 min in the dark with secondary anti-rabbit antibody
608 conjugated to fluorescein isithiocyanate (FITC) (Sigma, 1:500 dilution in PBS-T) and
609 washed three times with PBS-T. After dried, several drops of FluorSave (Calbiochem)
610 were added atop, covered with a coverslip and sealed with nail lack. Fluorescence was
611 imaged using a Leica DM6000B fluorescence microscope and an ORCA-ER camera
612 (Hamamatsu). Fluorescence was monitored using a FITC L5 filter (excitation, band-
613 pass (BP) 480/40 filter; emission, BP 527/30 filter). Images were analyzed using the
614 ImageJ software (http://imagej.nih.gov/ij).
615

Treatment with berberine

Cultures of wild-type *Anabaena* grown in BG11 medium and containing about 1 μg chlorophyll *a* ml^{-1} were incubated in the presence of 0.1 to 1 mM berberine hemisulphate (Sigma) at 30ºC for 24 to 72 h. After incubation, cells were harvested by centrifugation and the localization of FtsZ and SepJ was studied by immunofluorescence as described above.

BACTH complementation assays

Plasmids used for BACTH assays (Karimova *et al.*, 2005) were co-transformed into BTH101 (*cya*-99). The transformants were plated onto LB medium containing selective antibiotics, 40 μg ml^{-1} 5-bromo-4-chloro-3-indolyl-β-D-galactopyranoside (X-gal) and 0.5 mM IPTG and, then, incubated at 30ºC for 24 to 36 h. Efficiencies of interactions between different hybrid proteins were quantified by measuring β-galactosidase activity in liquid cultures. Bacteria were grown in LB medium in the presence of 0.5 mM IPTG and appropriate antibiotics at 30ºC for 16 h. Before the assays, the cultures were diluted 1:5 into buffer Z (60 mM Na_2HPO_4, 40 mM NaH_2PO_4, 10 mM KCl and 1 mM $MgSO_4$). To permeabilize cells, 30 μl of toluene and 35 μl of a 0.1% SDS solution were added to 2.5 ml of bacterial suspension. The tubes were vortexed for 10 s and incubated with agitation at 37ºC for 45 min for evaporation of toluene. For the enzymatic reaction, 875 μl of permeabilized cells were added to buffer Z supplemented with β-mercaptoethanol (25 mM final concentration), to a final volume of 3.375 ml. The tubes were incubated at 30ºC in a water bath for at least 5 min. The reaction was started by adding 875 μl of 0.4 mg ml^{-1} *o*-nitrophenol-β-galactoside (ONPG) in buffer Z without β-mercaptoethanol. 1-ml samples, taken at times up to 10 min, were added to 0.5 ml of 1 M Na_2CO_3 to stop the reaction. $A_{420\ nm}$ was recorded, and the amount of *o*-nitrophenol produced was

641 calculated using an extinction coefficient $\varepsilon_{420\ nm}$ = 4.5 mM^{-1} cm^{-1} and referred to the
642 amount of total protein, determined by a modified Lowry procedure (Markwell *et al.*,
643 1978). The *o*-nitrophenol produced per mg of protein versus time was represented, and
644 β-galactosidase activity was deduced from the slope of the linear function.
645

646 ## Acknowledgments

647 Research supported by grants no. BFU2011-22762 and BFU2013-44686-P from Plan
648 Nacional de Investigación, Spain, co-financed by the European Regional Development
649 Fund.
650

651 ## Conflict of interest

652 The authors declare that they have no conflict of interest.
653

654 ## References

655

656 Altendorf, K.H., and Staehelin, L.A. (1974) Orientation of membrane vesicles from
657 *Escherichia coli* as detected by freeze-cleave electron microscopy. *J Bacteriol*
658 **117**: 888-899.
659 Ausubel, F.M., Brent, R., Kingston, R.E., Moore, D.D., Seidman, J.G., Smith, J.A., and
660 Struhl, K. (2014) Current Protocols in Molecular Biology. New York: *Greene*
661 *Publishing and Wiley-Interscience.*
662 Bauer, C.C., Buikema, W.J., Black, K., and Haselkorn, R. (1995) A short-filament
663 mutant of *Anabaena* sp. strain PCC 7120 that fragments in nitrogen-deficient
664 médium. *J Bacteriol* **177**: 1520-1526.
665 Boberek, J.M., Stach, J., and Good, L. (2010) Genetic evidence for inhibition of
666 bacterial division protein FtsZ by berberine. *PLoS One* **5**: e13745.

667 Burnat, M., Herrero, A., and Flores, E. (2014) Compartmentalized cyanophycin
668 metabolism in the diazotrophic filaments of a heterocyst-forming cyanobacterium.
669 *Proc Natl Acad Sci USA* **111**: 3823-3828.
670 Cai, Y., and Wolk, C.P. (1990) Use of conditionally lethal gene in *Anabaena* sp. strain
671 PCC 7120 to select for double recombinants and to entrap insertion sequences. *J*
672 *Bacteriol* **172**: 3138-3145.
673 Cassier-Chauvat, C., and Chauvat, F. (2014) Cell division in cyanobacteria. In *The Cell*
674 *Biology of Cyanobacteria*. Flores, E., and Herrero, A. (eds). Norfolk, UK: Caister
675 Academic Press, pp 7-27.
676 Chen, J.C., Minev, M., and Beckwith, J. (2002) Analysis of ftsQ mutant alleles in
677 *Escherichia coli*: complementation, septal localization, and recruitment of
678 downstream cell division proteins. *J Bacteriol* **184**: 695-705.
679 Chen, J.C., Weiss, D.S., Ghigo, J.M., and Beckwith, J. (1999) Septal localization of
680 FtsQ, an essential cell division protein in *Escherichia coli*. *J Bacteriol* **181**: 521-
681 530.
682 Claessen, D., Rozen, D.E., Kuipers, O.P., Søgaard-Andersen, L., and van Wezel, G.P.
683 (2014) Bacterial solutions to multicellularity: a tale of biofilms, filaments and
684 fruiting bodies. *Nat Rev Microbiol* **12**: 115-124.
685 Doherty, H.M., and Adams, D.G. (1995) Cloning and sequence of *ftsZ* and flanking
686 regions from the cyanobacterium *Anabaena* PCC 7120. *Gene* **163**: 93-96.
687 Domadia, P.N., Bhunia, A., Sivaraman, J., Swarup, S., and Dasgupta, D. (2008)
688 Berberine targets assembly of *Escherichia coli* cell division protein FtsZ.
689 *Biochemistry* **47**: 3225-3234.
690 Egan, A.J., and Vollmer, W. (2013) The physiology of bacterial cell division. *Ann N Y*
691 *Acad Sci* **1277**: 8-28.
692 Elhai, J., Vepritskiy, A., Muro-Pastor, A.M., Flores, E., and Wolk, C.P. (1997)
693 Reduction of conjugal transfer efficiency by three restriction activities of
694 *Anabaena* sp. strain PCC 7120. *J Bacteriol* **179**: 1998-2005.
695 Elhai, J., and Wolk, C.P. (1988) A versatile class of positive-selection vectors base don
696 the nonviability of palindrome-containing plasmids that allows cloning into long
697 polylinkers. *Gene* **8**: 119-138.
698 Flaherty, B.L., Van Nieuwerburgh, F., Head, S.R., and Golden, J.W. (2011) Directional
699 RNA deep sequencing sheds new light on the transcriptional response of

Anabaena sp. strain PCC 7120 to combined-nitrogen deprivation. *BMC Genomics* **12**: 332.

Flores, E., and Herrero, A. (2010) Compartmentalized function through cell differentiation in filamentous cyanobacteria. *Nat Rev Microbiol* **8**: 39-50.

Flores, E., Herrero, A., Wolk, C.P., and Maldener, I. (2006) Is the periplasm continuous in filamentous multicelular cyanobacteria? *Trends Microbiol* **14**: 439-443.

Flores, E., Pernil, R., Muro-Pastor, A.M., Mariscal, V., Maldener, I., Lechno-Yossef, S., Fan, Q., Wolk, C.P., and Herrero, A. (2007) Septum-localized protein required for filament integrity and diazotrophy in the heterocyst-forming cyanobacterium *Anabaena* sp. strain PCC 7120. *J Bacteriol* **189**: 3884-3890.

Giddings, T.H., and Staehelin, L.A. (1978) Plasma membrane architecture of *Anabaena cylindrica*: occurrence of microplasmodesmata and changes associated with heterocyst development and the cell cycle. *Cytobiologie* **16**: 235-249.

Haselkorn, R. (2007) Heterocyst differentiation and nitrogen fixation in cyanobacteria. In *Associative and Endophytic Nitrogen-fixing Bacteria and Cyanobacterial Associations*. Elmerich, C., and Newton WE (eds). The Netherlands: Springer, pp 233-255.

Herrero, A., Muro-Pastor, A.M., and Flores, E. (2001) Nitrogen control in cyanobacteria. *J Bacteriol* **183**: 411-425.

Herrero, A., Picossi, S., and Flores, E. (2013) Gene expression during heterocyst differentiation. *Adv Bot Research* **65**: 281-329.

Huang, K.H., Durand-Heredia, J., and Janakiraman, A. (2013) FtsZ ring stability: of bundles, tubules, crosslinks, and curves. *J Bacteriol* **195**: 1859-1868.

Kaneko, T., Nakamura, Y., Wolk, C.P., Kuritz, T., Sasamoto, S., Watanabe, A., Iriguchi, M., Ishikawa, A., Kawashima, K., Kimura, T., Kishida, Y., Kohara, M., Matsumoto, M., Matsuno, A., Muraki, A., Nakazaki, N., Shimpo, S., Sugimoto, M., Takazawa, M., Yamada, M., Yasuda, M., and Tabata, S. (2001) Complete genomic sequence of the filamentous nitrogen-fixing cyanobacterium *Anabaena* sp. strain PCC 7120. *DNA Res* **8**: 205-213.

Karimova, G., Dautin, N., and Ladant, D. (2005) Interaction network among *Escherichia coli* membrane proteins involved in cell division as revealed by bacterial two-hybrid analysis. *J Bacteriol* **187**: 2233-2243.

732 Karimova, G., Pidoux, J., Ullmann, A., and Ladant, D. (1998) A bacterial two-hybrid
733 system based on a reconstituted signal transduction pathway. *Proc Natl Acad Sci*
734 *USA* **95**: 5752-5256.
735 Klint, J., Rasmussen, U., and Bergman, B. (2007) FtsZ may have dual roles in the
736 filamentous cyanobacterium *Nostoc*/*Anabaena* sp. strain PCC 7120. *J Plant*
737 *Physiol* **164**: 11-18.
738 Koksharova, O.A., and Wolk, C.P. (2002) A novel gene that bears a DnaJ motif
739 influences cyanobacterial cell division. *J Bacteriol* **184**: 5524-5528.
740 Kuhn, I., Peng, L., Bedu, S., and Zhang, C.-C. (2000) Developmental regulation of the
741 cell division protein FtsZ in *Anabaena* sp. strain PCC 7120, a cyanobacterium
742 capable of terminal differentiation. *J Bacteriol* **182**: 4640-4643.
743 Kumar, K., Mella-Herrera, R.A., and Golden, J.W. (2010) Cyanobacterial heterocysts.
744 *Cold Spring Harb Perspect Biol* **2**: a000315.
745 Lang, N.J., and Fay, P. (1971) The heterocysts of blue-green algae II. Details of
746 ultrastructure. *Proc R Soc Lond B* **178**: 193-203.
747 Lehner, J., Zhang, Y., Berendt, S., Rasse, T.M., Forchhammer, K., and Maldener, I.
748 (2011) The morphogene AmiC2 is pivotal for multicelular development in the
749 cyanobacterium *Nostoc punctiforme*. *Mol Microbiol* **79**: 1655-1669.
750 Lutkenhaus, J., Pichoff, S., and Du, S. (2012) Bacterial cytokinesis: From Z ring to
751 divisome. *Cytoskeleton* **69**: 778-790.
752 Mackinney, G. (1941) Absorption of light by chlorophyll solutions. *J Biol Chem* **140**:
753 315-322.
754 Marbouty, M., Saguez, C., Cassier-Chauvat, C., and Chauvat, F. (2009a)
755 Characterization of the FtsZ-interacting septal proteins SepF and Ftn6 in the
756 spherical-celled cyanobacterium *Synechocystis* strain PCC 6803. *J Bacteriol* **191**:
757 6178-6185.
758 Marbouty, M., Saguez, C., Cassier-Chauvat, C., and Chauvat, F. (2009b) ZipN, an
759 FtsA-like orchestrator of divisome assembly in the model cyanobacterium
760 *Synechocystis* PCC 6803. *Mol Microbiol* **74**: 409-420.
761 Margolin, W. (2009) Sculpting the bacterial cell. *Curr Biol* **19**: R812-22.
762 Mariscal, V., and Flores, E. (2010) Multicellularity in a heterocyst-forming
763 cyanobacterium: pathways for intercellular communication. *Adv Exp Med Biol*
764 **675**: 123-135.

765 Mariscal, V., Herrero, A., and Flores, E. (2007) Continuous periplasm in a filamentous,
766 heterocyst-forming cyanobacterium. *Mol Microbiol* **65**: 1139-1145.
767 Mariscal, V., Herrero, A., Nenninger, A., Mullineaux, C.W., and Flores, E. (2011)
768 Functional dissection of the three-domain SepJ protein joining the cells in
769 cyanobacterial trichomes. *Mol Microbiol* **79**: 1077-1088.
770 Markwell, M.A.K., Hass, S.M., Bieber, L.L., and Tolbert, N.E. (1978) A modification
771 of the Lowry procedure to simplify protein determination in membrane and
772 lipoprotein samples. *Anal Biochem* **87**: 206-210.
773 Merino-Puerto, V., Mariscal, V., Mullineaux, C.W., Herrero, A., and Flores, E. (2010)
774 Fra proteins influencing filament integrity, diazotrophy and localization of septal
775 protein SepJ in the heterocyst-forming cyanobacterium *Anabaena* sp. *Mol*
776 *Microbiol* **75**: 1159-1170.
777 Merino-Puerto, V., Schwarz, H., Maldener, I., Mariscal, V., Mullineaux, C.W., Herrero,
778 A., and Flores, E. (2011) FraC/FraD-dependent intercellular molecular exchange
779 in the filaments of a heterocyst-forming cyanobacterium, *Anabaena* sp. *Mol*
780 *Microbiol* **82**: 87-98.
781 Merino-Puerto, V., Herrero, A., and Flores, E. (2013) Cluster of genes that encode
782 positive and negative elements influencing filament length in a heterocyst-
783 forming cyanobacterium. *J Bacteriol* **195**: 3957-3966.
784 Miyagishima, S., Wolk, C.P., and Osteryoung, K.W. (2005) Identification of
785 cyanobacterial cell division genes by comparative and mutational analyses. *Mol*
786 *Microbiol* **56**: 126-143.
787 Mohamed, A., and Jansson, C. (1989) Influence of light on accumulation of
788 photosynthesis-specific transcripts in the cyanobacterium *Synechocystis* 6803.
789 *Plant Mol Biol* **13**: 693–700.
790 Mullineaux, C.W., Mariscal, V., Nenninger, A., Khanum, H., Herrero, A., Flores, E.,
791 and Adams, D.G. (2008) Mechanism of intercellular molecular exchange in
792 heterocyst-forming cyanobacteria. *EMBO J* **27**: 1299-1308.
793 Muro-Pastor, A.M., Valladares, A., Flores, E., and Herrero, A. (2002) Mutual
794 dependence of the expression of the cell differentiation regulatory protein HetR
795 and the global nitrogen regulator NtcA during heterocyst development. *Mol*
796 *Microbiol* **44**: 1377-1385.
797 Natale, P., Pazos, M., and Vicente, M. (2013) The *Escherichia coli* divisome: born to
798 divide. *Environ Microbiol* **15:** 3169–3182.

799 Nayar, A.S., Yamaura, H., Rajagopalan, R., Risser, D.D., and Callahan, S.M. (2007)
800 FraG is necessary for filament integrity and heterocyst maturation in the
801 cyanobacterium *Anabaena* sp. strain PCC 7120. *Microbiology* **153**: 601-603.
802 Nürenberg, D.J., Mariscal, V., Parker, J., Mastroianni, G., Flores, E., and Mullineaux,
803 C.W. (2014) Branching and intercellular communication in the Section V
804 cyanobacterium *Mastigocladus laminosus*, a complex multicelular prokaryote.
805 *Mol Microbiol* **91**: 935-949.
806 Pfaffl, M.W. (2001) A new mathematical model for relative quantification in real-time
807 RT-PCR. *Nucleic Acids Res* **29**: e45.
808 Picossi, S., Flores, E., and Herrero, A. (2014) ChIP analysis unravels an exceptionally
809 wide distribution of DNA binding sites for the NtcA transcription factor in a
810 heterocyst-forming cyanobacterium. *BMC Genomics* **15**: 22.
811 Prentki, P., and Krisch, H.M. (1984) In vitro insertional mutagenesis with a selectable
812 DNA fragment. *Gene* **29**: 303-313.
813 Rippka, R., Deruelles, J., Waterbury, J.B., Herdman, M., and Stanier, R.Y. (1979)
814 Generic assignments, strain stories and properties of pure cultures of
815 cyanobacteria. *J Gen Microbiol* **111**: 1-61.
816 Sakr, S., Jeanjean, R., and Zhang, C.-C. (2006) Relationship among several key cell
817 cycle events in developmental cyanobacterium *Anabaena* sp. strain PCC 7120. *J*
818 *Bacteriol* **188**: 5958-5965.
819 Vicente, M., Rico, A.I., Martínez-Arteaga, R., and Mingorance, J. (2006) Septum
820 enlightenment: assembly of bacterial division proteins. *J Bacteriol* **188**: 19-27.
821 van den Ent, F., Vinkenvleugel, T.M., Ind, A., West, P., Veprintsev, D., Nanninga, N.,
822 den Blaauwen, T., and Löwe, J. (2008) Structural and mutational analysis of the
823 cell division protein FtsQ. *Mol Microbiol* **68**: 110-123.
824 Villanelo, F., Ordenes, A., Brunet, J., Lagos, R., and Monasterio, O. (2011) A model for
825 the *Escherichia coli* FtsB/FtsL/FtsQ cell division complex. *BMC Struct Biol* **11**:
826 28.
827 Wilk, L., Strauss, M., Rudolf, M., Nicolaisen, K., Flores, E., Kühlbrandt, W., and
828 Schleiff, E. (2011) Outer membrane continuity and septosome formation between
829 vegetative cells in the filaments of *Anabaena* sp. PCC 7120. *Cell Micriobiol* **13**:
830 1744-1754.
831 Wolk, C.P. (1996) Heterocyst formation. *Annu Rev Genet* **30:** 59–78.

832 Wolk, C.P., Ernst, A., and Elhai, J. (1994) Heterocyst metabolism and development. In
833 *The molecular biology of cyanobacteria*. Bryant, D.A. (ed). Dordrecht: Kluwer
834 Academic Publishers, pp 769–823.
835 Zhang, C.-C., Huguenin, S., and Friry, A. (1995) Analysis of genes encoding the cell
836 division protein FtsZ and a glutathione synthetase homologue in the
837 cyanobacterium *Anabaena* sp. PCC 7120. *Res Microbiol* **146**: 445-455.

838

839 **Figure legends**

840

841 **Fig. 1.** Genomic structure and phenotype of *Anabaena* sp. strain CSFR18 (C.S3-P_{ND}-
842 *ftsZ*). (A) Schematic (not to scale) of the *ftsQ-ftsZ* genomic region in strain CSFR18,
843 including, shown in blue color, the sequence of the DNA fragment bearing the
844 introduced synthetic NtcA-dependent promoter: blue bracket, NtcA-binding site; red
845 bracket, -10 promoter hexamer; black arrow, predicted transcription start site. Sequence
846 in red corresponds to the end of C.S3 and sequence in green to the *ftsZ* 5' and upstream
847 region (the three first codons of the gene are underlined). C.S3 includes the Ω cassette
848 that encodes resistance to Sm and Sp (gene orientation indicated by the white arrow)
849 and bears transcriptional terminators in both ends, indicated by white exes (Elhai and
850 Wolk, 1988). (B) Test of growth on solid media. Samples from BG11-grown filaments
851 of strains PCC 7120 (wild type) and CSFR18 were spotted at different dilutions in solid
852 media with the indicated nitrogen source, incubated under growth conditions and
853 photographed after 7 days. (C, D) Cultures of BG11-grown filaments of the indicated
854 strains were incubated under growth conditions in liquid media with the indicated
855 nitrogen sources and visualized by light microscopy after 5 days (C) or photographed
856 after 7 days (D). Size bars in C, 3 μm. The area of the cells was determined in the
857 different liquid cultures with the following results: nitrate-containing cultures, 12.51 ±
858 0.53 μm^2 for the wild type and 22.9 ± 1.14 μm^2 for the mutant; ammonium-containing
859 cultures, 13.36 ± 0.68 μm^2 for the wild type and 45.37 ± 3.61 μm^2 for the mutant;
860 cultures without combined nitrogen, 12.18 ± 0.33 μm^2 for the wild type and 10.9 ± 0.50
861 μm^2 for the mutant (37 cells for each strain and growth condition were measured).
862 Student's *t* test indicated that the differences between the mutant and the wild type were
863 significant in the cultures containing nitrate ($P < 10^{-11}$) or ammonium ($P < 10^{-12}$).

Fig. 2. Expression of *ftsZ* in *Anabaena* strains PCC 7120 (wild type) and CSFR18 (C.S3-P_{ND}-*ftsZ*). (A) Levels of *ftsZ* transcript in strains CSFR18 and PCC 7120, relative to those in nitrate-grown PCC 7120 (wild type) cells. RNA was isolated from BG11-grown filaments incubated for 48 hours under culture conditions with the indicated nitrogen source, and RT-qPCR was performed as described in Experimental procedures. (B) Western blot analysis of FtsZ. BG11-grown filaments of the indicated strain were incubated for 48 hours under culture conditions with the indicated nitrogen source, and extracts were prepared, loaded into SDS-PAGE gels (60 µg protein per lane), electrophoresed and probed with antibodies raised against the *Anabaena* FtsZ protein as described in Experimental procedures.

Fig. 3. Immunofluorescence localization of FtsZ in *Anabaena* strains PCC 7120 (wild type) and CSFR18 (C.S3-P_{ND}-*ftsZ*). BG11-grown filaments of the indicated strain were incubated for 48 hours under culture conditions with the indicated nitrogen source, prepared for immunofluorescence analysis with anti *Anabaena* FtsZ protein antibodies, and visualized by fluorescence microscopy as described in Experimental procedures. Arrows point to heterocysts. Size bar, 3 µm; magnification was the same for all micrographs. Merged bright-field and fluorescence images are shown.

Fig. 4. Immunofluorescence localization of SepJ in *Anabaena* strains PCC 7120 (wild type) and CSFR18 (C.S3-P_{ND}-*ftsZ*). BG11-grown filaments of the indicated strain were incubated for 48 h under culture conditions with the indicated nitrogen source, prepared for immunofluorescence analysis with antibodies raised against the coiled-coil domain of the *Anabaena* SepJ protein, and visualized by fluorescence microscopy as described

889 in Experimental procedures. Size bars, 3 μm. Arrowheads point to places, in dividing
890 cells, where the immunofluorescence signal is in a position similar to that of a Z ring.
891 Bright-field, fluorescence (SepJ) and merged images are shown.
892
893 **Fig. 5.** FtsZ and SepJ localization in berberine-treated *Anabaena* filaments. Filaments
894 grown in BG11 medium were treated (+) or not (-) with 0.1 mM berberine for 24 h and
895 subjected to immunofluorescence analysis with anti FtsZ and anti SepJ-CC antibodies
896 as described in Experimental procedures. Size bar, 3 μm; magnification was the same
897 for the four micrographs. Merged bright-field and fluorescence images are shown
898
899 **Fig. 6.** Schematic of the protein fusions used in BACTH analysis. The T25 and T18
900 fragments of the catalytic subunit of adenylate cyclase are represented as block arrows
901 indicating the orientation (N-terminal to C-terminal) of the polypeptide. The SepJ
902 protein (751 amino acid residues; blue) consists of three domains: N-terminal coiled-
903 coil domain (CC), linker and C-terminal permease (likely containing 9 or 11
904 transmembrane segments). *Anabaena* FtsQ (281 amino acid residues; green) is
905 predicted to contain the same domains as *E. coli* FtsQ: an N-terminal transmembrane
906 segment and periplasmic α (POTRA) and β domains (van den Ent *et al.*, 2008).
907 *Anabaena* FtsZ (428 amino acid residues; yellowish) is a predicted soluble protein.
908 *Anabaena* FtsW (396 amino acid residues; red) is predicted to have 8 transmembrane
909 segments with its N- and C-termini in the cytoplasmic side of the cytoplasmic
910 membrane. N denotes the N-terminus in each fusion protein.
911
912

Fig. 7. Joint extraction from *E. coli* of SepJ-GFP and His_6-tagged *Anabaena* FtsQ. Total extracts from cells of *E. coli* expressing SepJ-GFP or Δpp-SepJ-GFP and/or His_6-tagged *Anabaena* FtsQ were allowed to interact with anti-GFP MicroBeads and loaded into a MACS column, and the retained material was then eluted and subject to SDS-PAGE. Tagged *Anabaena* FtsQ (about 33 kDa) was identified using an anti-pentahistidine antibody (A), and tagged SepJ was identified using an anti-GFP antibody (B). For each lane the proteins expressed in the corresponding *E. coli* strain are shown: SepJ refers to SepJ-GFP; Δpp, SepJ-GFP without most of the predicted SepJ periplasmic section; FtsQ, His_6-tagged *Anabaena* FtsQ. ϕ, plasmid vector without insert. White triangles point to signals corresponding to the SepJ-GFP fusion protein (about 108 kDa) and black triangles point to Δpp-SepJ-GFP (about 68 kDa). The SepJ protein generates forms moving to different extents in SDS-PAGE gels (Mariscal *et al.*, 2011). Some degradation of the SepJ-GFP fusion proteins releasing at least two forms of GFP (about 27 kDa) and, in the case of the complete protein, possibly also a protein lacking the predicted periplasmic section appears to have taken place.

930

T18 fusion	T25 fusion	β-Galactosidase activity (nmol ONP [mg protein]$^{-1}$ min^{-1})	Student's *t* test
		Mean ± SD (n)	*P*
Negative control			
T18	T25	9.70 ± 2.06 (8)	
SepJ self-interactions			
T18	SepJ-T25	9.35 ± 1.38 (8)	0.6969
SepJ-T18	T25	10.04 ± 2.45 (8)	0.7705
SepJ-T18	SepJ-T25	199.47 ± 57.95 (7)	4 E-07 (*)
T18	SepJ(ΔTM)-T25	10.76 ± 0.63 (4)	0.3489
T18	SepJ(Δpp)-T25	12.05 ± 1.81 (4)	0.0829
T18	SepJ(Δlinker)-T25	9.76 ± 1.10 (4)	0.9589
T18	SepJ(ΔCC)-T25	12.44 ± 1.65 (4)	0.0443
SepJ(ΔTM)-T18	T25	10.18 ± 4.17 (6)	0.7791
SepJ(Δpp)-T18	T25	9.32 ± 2.09 (6)	0.7395
SepJ(Δlinker)-T18	T25	10.51 ± 4.25 (6)	0.6431
SepJΔCC)-T18	T25	11.47 ± 3.74 (6)	0.2791
SepJ(ΔTM)-T18	SepJ(ΔTM)-T25	14.33 ± 4.34 (4)	0.0278
SepJ(ΔTM)-T18	SepJ-T25	11.85 ± 1.89 (4)	0.1110
SepJ-T18	SepJ(ΔTM)-T25	15.16 ± 5.36 (4)	0.0256
SepJ(Δpp)-T18	SepJ(Δpp)-T25	16.69 ± 1.81 (4)	0.0002 (*)
SepJ(Δpp)-T18	SepJ-T25	11.48 ± 1.41 (4)	0.1548
SepJ-T18	SepJ(Δpp)-T25	11.27 ± 2.02 (4)	0.2399
SepJ(Δlinker)-T18	SepJ(Δlinker)-T25	25.50 ± 3.39 (4)	1 E-06 (*)
SepJ(Δlinker)-T18	SepJ-T25	45.16 ± 9.31 (4)	8 E-07 (*)
SepJ-T18	SepJ(Δlinker)-T25	73.83 ± 14.08 (3)	2 E-07 (*)
SepJ(ΔCC)-T18	SepJ(ΔCC)-T25	154.65 ± 30.36 (3)	1 E-07 (*)
SepJ(ΔCC)-T18	SepJ-T25	69.36 ± 16.90 (3)	3 E-06 (*)
SepJ-T18	SepJ(ΔCC)-T25	74.01 ± 17.07 (4)	6 E-07 (*)
SepJ-divisome protein interactions			
T18	FtsZ-T25	8.51 ± 1.70 (4)	0.3451
T18	T25-FtsW	9.30 ± 1.19 (4)	0.7298
T18	T25-FtsQ	8.69 ± 2.32 (6)	0.4053
SepJ-T18	FtsZ-T25	7.50 ± 1.53 (4)	0.0903
SepJ-T18	T25-FtsW	28.68 ± 23.14 (4)	0.0359
SepJ-T18	T25-FtsQ	207.50 ± 118.67 (5)	0.0005 (*)
SepJ(ΔTM)-T18	T25-FtsQ	10.34 ± 1.86 (4)	0.6161
SepJ(Δpp)-T18	T25-FtsQ	15.64 ± 5.42 (4)	0.0181
SepJ(Δlinker)-T18	T25-FtsQ	10.18 ± 4.00 (3)	0.7930
SepJ(ΔCC)-T18	T25-FtsQ	161.87 ± 50.86 (4)	5 E-06 (*)
T18	T25-FtsQ(Δα)	5.72 ± 4,01 (2)	0,0680
T18	T25-FtsQ(Δβ)	7.14 ± 4.49 (2)	0.2298
SepJ-T18	T25-FtsQ(Δα)	15.10 ± 8.48 (4)	0.1057
SepJ-T18	T25-FtsQ(Δβ)	302.06 ± 121.31 (3)	4 E-05 (*)

Table 1. Quantification of SepJ self-interactions and interactions between SepJ and some divisome proteins assessed by BACTH.

931
932

The interactions of the proteins fused to the T18 and T25 vectors cloned in *E. coli* were measured as β-galactosidase activity in liquid cultures as described in Experimental procedures. The protein fused to the N- or the C-terminus of T18 or T25 is indicated in each case (N-terminus, protein-T18 or protein-T25; C-terminus, T18-protein or T25-protein). Non-fused T18/T25 plasmid pair was used as negative control. A T18-zip/T25-zip positive control produced an activity of about 600 nmol ONP (mg protein)$^{-1}$ min^{-1}. The mean and standard deviation of the results from the number of experiments indicated (n) is presented. The difference between each plasmid combination and the T18/T25 plasmid pair was assessed by the Student's *t* test (*P* indicated in each case); an asterisk (*) highlights differences significant at $P \leq 0.0005$.

Fig. 1

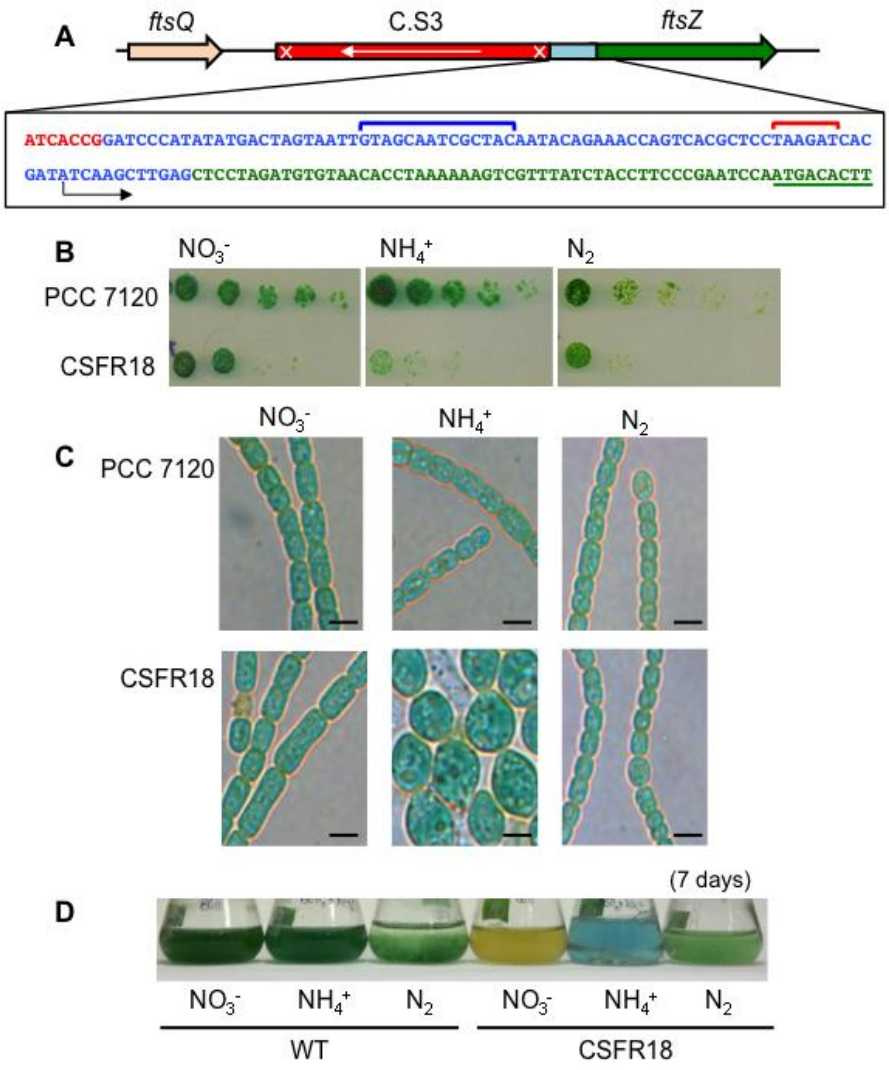

933
934 MMI_12956_F1
935

Fig. 2

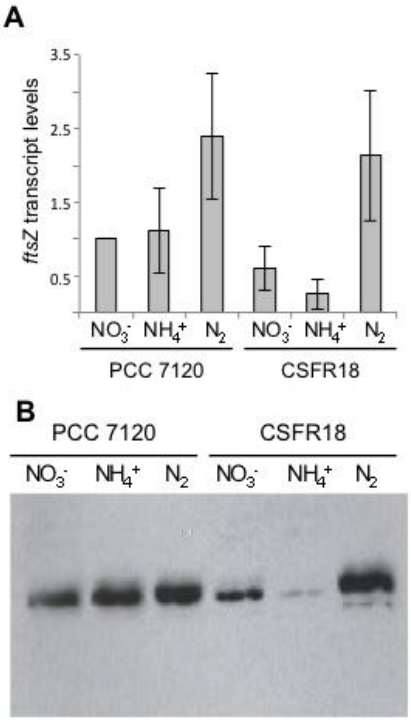

936
937 MMI_12956_F2
938

Fig. 3

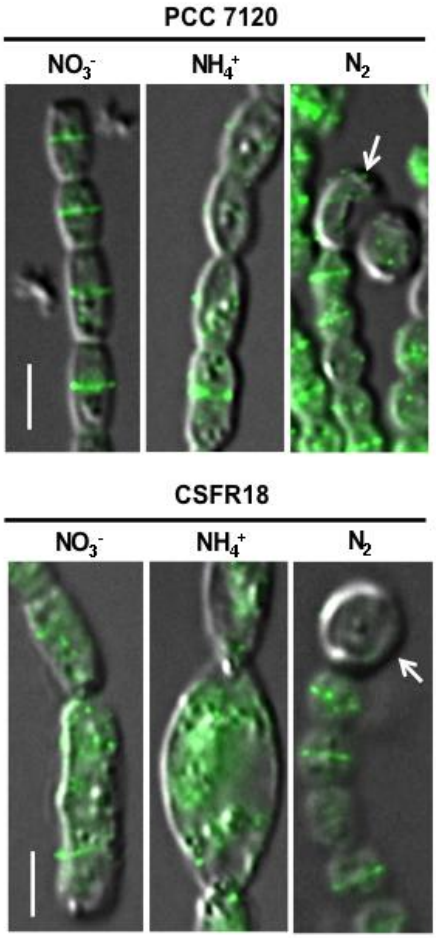

939
940 MMI_12956_F3
941

Fig. 4

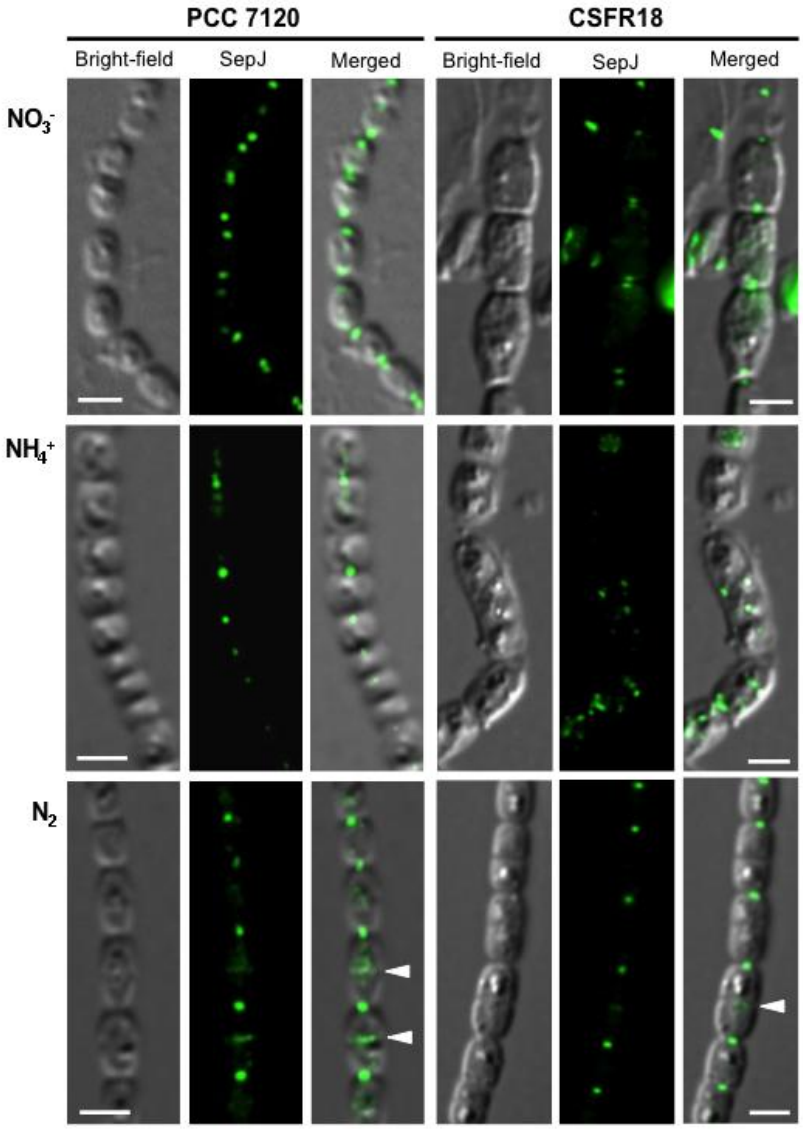

942
943
944

MMI_12956_F4

Fig. 5

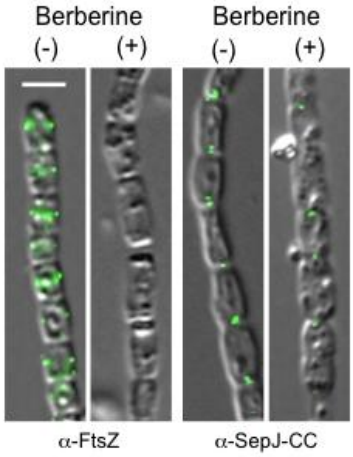

945
946 MMI_12956_F5
947

Fig. 6

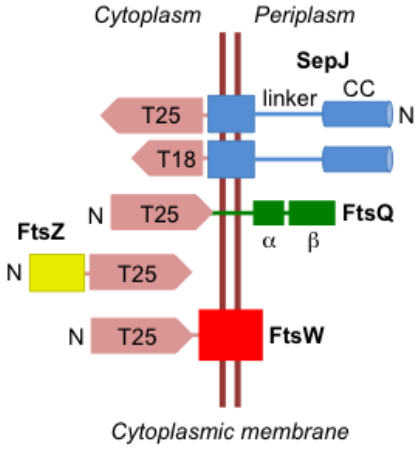

948
949
950

MMI_12956_F6

Fig. 7

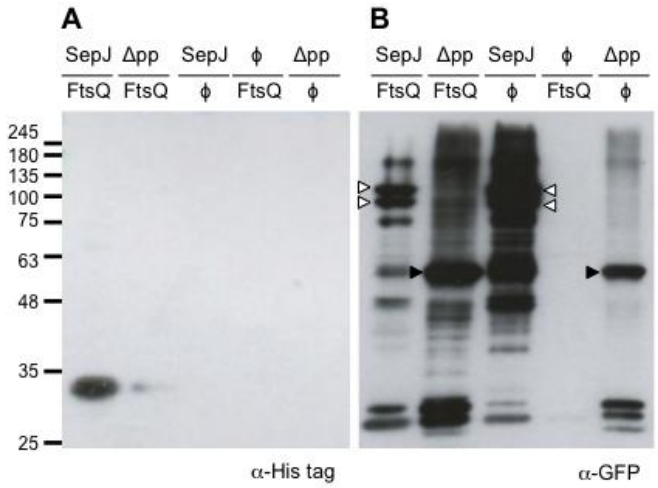

MMI_12956_F7

De: molmicro@dundee.ac.uk
Asunto: Molecular Microbiology - MMI-2014-14449.R2
Fecha: 30 de enero de 2015, 16:55
Para: eflores@ibvf.csic.es

M

30-Jan-2015

Re: Molecular Microbiology - MMI-2014-14449.R2

Dear Enrique,

I am happy to tell you that your manuscript entitled Divisome-dependent subcellular localization of cell-cell joining protein SepJ in the filamentous cyanobacterium Anabaena has been accepted for publication in Molecular Microbiology without further review. I have also requested that your colour fees be waived as agreed previously.

OnlineOpen is available to authors of articles who wish to make their article open access. With OnlineOpen the author, their funding agency, or institution pays a fee to ensure that the article is made available to non-subscribers upon publication via Wiley Online Library, as well as deposited in PubMed Central and PMC mirror sites. In addition to publication online via Wiley Online Library, authors of OnlineOpen articles are permitted to post the final, published PDF of their article on a website, institutional repository, or other free public server, immediately on publication. If you want your article to be open access please choose the appropriate license agreement when you log in to Wiley's Author Services system. Click on 'Make my article OnlineOpen' and choose the appropriate license by clicking on 'Sign license agreement now' on Wiley's Author Services system. Commissioned papers are made available free on line without charge to authors, but the publisher retains the copyright and license.

By submitting this manuscript for publication you confirm that, if applicable, this work has been prepared in accordance with the NSABB guidelines for publication of dual use life sciences research (see Author Guidelines).

IMPORTANT: To ensure full compliance with NIH requirements, accepted manuscripts from authors funded by the NIH will be uploaded automatically and free of charge into the PMC data base one year after publication. The NIH has approved this measure.

In order for the publishers to handle the manuscript efficiently, we have forwarded the materials you supplied to the publisher for immediate production by Wiley.

PLEASE NOTE: Your article cannot be published until you have signed the appropriate license agreement. Within the next few days you will receive an e-mail from Wiley's Author Services system which will ask you to log in and will present you with the appropriate license for completion.

You must also return a completed and signed Color Work Agreement Form (available from http://onlinelibrary.wiley.com/store/10.1111/(ISSN)1365-2958/asset/homepages/MMI_SN_Sub2000_F_CoW.pdf?v=1&s=045703b9e6bda5909cf5bab8fd86654fc35e1dbb&isAguDoi=false) if your article contains ANY color artwork, even if the material is to be published without cost to you (as is the case for all commissioned articles). If you would like to publish the figures in color both in print and online, an original signed hardcopy MUST be mailed to the address below. If however you would like to set your articles as colour online only or in the case of commissioned articles, electronic/faxed copies of the signed Color Work Agreement Form will be accepted. You may email the completed form to the Production Editor.

THE ACCEPTANCE DATE WILL BE THE DATE THAT ALL THE ABOVE IS RECEIVED AT THE PRODUCTION OFFICE. THEREFORE IT IS ESSENTIAL THAT ALL THE REQUIRED MATERIAL IS SENT IN A SINGLE PACKAGE. PUBLICATION WILL ONLY PROCEED ON RECEIPT OF THIS MATERIAL.

Please mail/courier all completed and signed Colour Work Agreement forms to:

Customer Services (OPI)
John Wiley & Sons Ltd, European Distribution Centre
New Era Estate
Oldlands Way
Bognor Regis
West Sussex
PO22 9NQ

From now on handling of the manuscript will be undertaken by the production office. Any correspondence relating to proofs, etc, should be e-mailed directly to the production editor at mmi@wiley.com.

The production office will send you an alert containing a link to a web site approximately 4 weeks after receipt of all material. The proof of your article can be downloaded as a PDF file from this site. Acrobat Reader will be required in order to read this file. This software can be downloaded (free of charge) from the following Web site:
http://www.adobe.com/products/acrobat/readstep2.html
This will enable the file to be opened, read on screen, and printed out in order for any corrections to be added. Further instructions will be sent with the proofs. Proofs will be posted if no e-mail address is available; in your absence, please arrange for a colleague to access your e-mail to retrieve the proofs and let the Production Editor know of an alternative

arrange for a colleague to access your e-mail to retrieve the proofs and let the Production Editor know of an alternative contact point.

Publication will normally be within five weeks of receipt of your corrected proofs.

The manuscript that I have accepted today is the final version: only errors introduced by the copy-editor or typesetter can be corrected on the proofs. Any requests for changes to the data or the text will cause the paper to be referred back to me, and possibly to the referees, and will delay publication of your article.

Once again, thank you for submitting your paper to Molecular Microbiology. I hope you will submit future papers to the journal.

With best wishes,

Tracy

Tracy Palmer
Division of Molecular Microbiology
College of Life Sciences
University of Dundee
DUNDEE DD1 5EH
Scotland

Phone 01382 386464
Fax 01382 388216